REGULATION OF SURFACE TOPOGRAPHY OF MOUSE PERITONEAL CELLS

Formation of Microvilli and Vesiculated Pits on Omental Mesothelial Cells by Serum and Other Proteins

LAIRD D. MADISON, BEVERLY BERGSTROM-PORTER, ANTHONY R. TORRES, and EMMA SHELTON

From the Laboratory of Biochemistry, National Cancer Institute, National Institutes of Health, Bethesda, Maryland 20205

ABSTRACT

The mesothelial cells of the mouse omentum provide an in vivo model for the study of the mobilization of labile microvilli on the cell surface. These mesothelial cells are sparsely covered with microvilli and large pits 150–400 nm in diameter, termed vesiculated pits. On the unstimulated cell, the microvilli average 44/100 μm^2 and pits, 30/100 μm^2 of surface and they are rapidly induced to increase in number by the intraperitoneal injection of isologous mouse serum. After 2 min, microvilli increase threefold, continue to sevenfold at 30 min, and decrease to fourfold at 90 min. Vesiculated pits increase with similar kinetics. Bovine serum albumin and gamma globulin also stimulate the microvilli and pits to form, but the response is a slow, gradual rise to five- or sixfold the normal value at 90 min. Evidence indicates that multiple factors, possibly including insulin and immunoglobulins, are involved in the effect of serum.

The close physical and temporal relationship between microvilli and pits suggests that a correlation exists in their mobilization by the cell and it is hypothesized that microvilli function in the regulation of the cortical microfilament network in effecting this mobilization.

KEY WORDS microvilli · vesiculated pits · cell surface topography · omental mesothelial cell

Microvilli are common and outstanding features of the cell surface. They can be present as stable, differentiated structures in the case of the brush border of the intestine (12, 20) or as labile, dynamic structures in the case of connective, lymphatic, or mesothelial cells (3, 23). Although it is reasonable to assume that the stable microvilli of the brush border function to increase membrane transport, the reasons for the presence of labile microvilli on a wide variety of functionally different cell types have not been satisfactorily explained nor has the control of their mobilization by the cell been studied. It has been suggested that these microvilli act as a site of membrane reserve for cell movement and division (10, 15), as a means of protective entrapment of glycocalyx on serosal surfaces (3), or to increase the surface area without increasing volume to enhance membrane transport (21). Cells in culture have served as models to

show that the presence of microvilli on the surface of different cells can be modulated by dibutyryl cAMP (26, 33), insulin (11), stage in mitotic cycle (25), cell culture density (22, 29), or substitution of galactose, xylose, or mannose for glucose in the growth medium (2). To our knowledge, modulation of microvilli on cells in vivo has not been reported nor has the kinetics of the appearance of microvilli in response to stimulus been studied in any system.

The omentum of the mouse (13, 14) is an excellent tissue for the study of induced changes in the cell surface. It is bathed with a small quantity of peritoneal fluid that is low in protein relative to blood serum and it is covered with flat mesothelial cells that are sparsely endowed with microvilli and vesiculated pits in the normal condition. These surface features, as seen by scanning and transmission electron microscopy, are profoundly affected when the ambient protein concentration in the peritoneal space is raised.

Presented here is a description of these changes and their quantitation. These results provide a basis for future study of the involvement of the cytoskeleton in the control of the topography of the cell surface.

MATERIALS AND METHODS

Materials

Strain A (A/LN × A/He) female mice between 2 and 6 mo of age were used in all experiments. Isologous normal mouse serum (NMS), with or without heat inactivation at 57°C for 30 min, normal human serum, normal Sprague-Dawley rat serum, rabbit serum, type 15Q heat-inactivated, strain 13 guinea pig serum, and fetal calf serum (Grand Island Biological Co., Grand Island, N. Y.) were used. All serums were stored frozen and were filtered through a 0.22-μm Millipore filter (Millipore Corp., Bedford, Mass.) immediately before intraperitoneal (i.p.) injection with a 25-gauge, 5/8-inch needle. Bovine serum albumin (BSA), fraction V (Miles Pentex, Kankakee, Ill., lot No. 194) was dissolved in phosphate-buffered saline (PBS) to a concentration of 1, 4.7, 5.6, and 50 mg/ml and filtered before use. Bovine gamma globulin (BGG), fraction II (Miles Pentex Lot No. 46) was dissolved in PBS at a concentration of 50 mg/ml and filtered before use. The protein concentration of NMS was determined to be 5.6 mg/ml by the method of Lowry et al. (19). In the NMS dilution experiments, PBS was used to make 2, 10, 20, and 50% solutions of normal serum. Purified human α_2-macroglobulin (kindly supplied by Dr. Ira Pastan), mouse myeloma proteins IgG (γ1k), IgMk, and IgAk (kindly supplied by Dr. Michael Potter) were dissolved in PBS at a concentration of 1 mg/ml and filtered before use. Insulin (Bovine, Elanco Products Co., Indianapolis, Ind., lot No. 8K430D) at 5 μg/ml and human low-density lipoprotein (LDL, kindly supplied by Dr. Brian Brewer) at 200 μg/ml were prepared in PBS containing 1 mg/ml BSA as a carrier. Glucose was dissolved in PBS to give solutions ranging from 10 to 110 mM. For one experiment, 3 ml of NMS was dialyzed at 4°C for 24 h against four changes of 500 ml of PBS. Glutaraldehyde, 2.5% diluted from 50% (Tousimis, Rockville, Md.), was prepared in 0.035 M cacodylate buffer containing 2% sucrose, pH 7.4, for omentums fixed for transmission electron microscopy or in PBS for omentums fixed for scanning electron microscopy. 1% osmium tetroxide was prepared in cacodylate buffer as described above.

Fractionation and Electrophoresis of NMS

DEAE-cellulose (DE-52) and CM-cellulose (CM-52) were obtained from Whatman Inc. Columns were packed under air pressure rising at 10 lb^2 and were pumped at 20 ml/h. An LKB IV (LKB Instruments, Inc., Rockville, Md.) monitored the column effluent at 280 nm.

Mouse serum (11 ml), which had been dialyzed overnight against 2 vol of distilled water, was pumped onto a 6.6-ml glass column (14 × 7 cm) packed with DE-52 equilibrated with 10 mM sodium phosphate, pH 7.0. The column was washed free of unadsorbed protein with 50 mM sodium phosphate, pH 7.0, and the adsorbed proteins were eluted with 0.5 M sodium dihydrogen phosphate. Under these conditions ~20% of the serum protein was adsorbed to the column. The pass-through (30 ml) from the DEAE-cellulose column was adjusted to pH 5.9 by the addition of 0.5 M sodium dihydrogen phosphate. The sample was then centrifuged to pellet the precipitate, and the clear supernate was applied to a 6.6-ml column of CM-52 equilibrated with 10 mM sodium phosphate, pH 6.1. The column was washed free of unadsorbed protein with 10 mM sodium phosphate, pH 6.1, and the adsorbed proteins were eluted with 0.2 M disodium phosphate.

The discontinuous polyacrylamide gel system of Davis (8) was used for electrophoresis of the serum and column fractions. Each sample applied to the slab gel (75 × 175 × 2 mm) was a mixture of 7 μl of 30% sucrose and 10–43 μl of dialyzed serum or column fractions. The gel was stained with Coomassie Brilliant G-250 (28) after electrophoresis at 200 V and 40 mA for 2 h.

Specimen Preparation

Mice, shaven on the ventral surface, were injected i.p. with 0.5 ml of the appropriate stimulant at room temperature. At intervals thereafter, they were sacrificed by CO_2 intoxication and exsanguination, fixative was injected i.p., and the animals were manipulated to distrib-

ute the fixative. To recover omentums at the 2-min postinjection interval, mice were sacrificed immediately and the fixative was injected at 2 min. For other time periods, the animals were left alive and quiet until 2 min before the chosen fixation time. After *in situ* fixation for 2 min, the omentum, with attached fat strip and pancreatic lobe connections, was removed and placed in fresh fixative for 20 min at room temperature or for up to 24 h at 4°C for scanning electron microscopy. For transmission electron microscopy, after 20-min fixation at room temperature the omentums were washed in cacodylate buffer and postfixed in 1% OsO_2 for 30 min.

For scanning electron microscopy, samples were dehydrated through ethanol and chloroform, critical-point dried out of liquid CO_2, and rotary-shadowed with carbon and gold-palladium. The omentums were examined and photographed with a JEOL JSM-35U SEM equipped with an LaB_6 electron gun operating at 25 kV. Specimens were photographed with 35–45° tilt for surface detail or at 0° tilt for use in quantitative analysis of the cell surface. For transmission electron microscopy, the omentums were stained en bloc in 0.5% aqueous uranyl acetate, dehydrated, and flat-embedded in Epon. *En face* and cross sections (80 nm) were stained in 0.5% aqueous uranyl acetate and 0.2% lead citrate, and examined and photographed in a Siemens 101 electron microscope equipped with a 50-m objective aperture and operated at 80 kV.

SEM Photography for Quantitative Analysis of the Cell Surface

To assure an unbiased sampling of the tissues for each time period, a regime of random-shot photography was followed. Areas of mesothelial cells between large fenestrations (Fig. 1) and large enough to fill an entire × 6,000 or 7,800 field of the microscope were selected at a magnification of 600 or 780 with 0° tilt of the specimen. At this magnification, regions of cell junctions and areas of extreme convolution could be discerned without clear visualization of the microvillus density. Both regions of cell junction and convolution were rejected because of the error introduced in calculating the number of microvilli per unit area and surface area photographed. When a satisfactory area was located, the magnification was briefly increased to 60,000 or 78,000 to accomplish critical focusing on the cell surface. The magnification was then decreased to 6,000 or 7,800 and a photograph was taken without further orientation or selection of the image. Five photographs representing areas from the four corners and the middle of each omentum were recorded. It is believed that this procedure eliminated any biased photographic sampling of the tissue specimens.

Quantitation of Microvillus and Pit Density

Either the original Polaroid prints or × 2.4 enlarged prints from the original negative were used for quantitative study. An area corresponding to 100 μm^2 was selected by overlaying a 1/8-inch-thick clear plastic sheet with an appropriate area inscribed on it. Counts were made of microvilli and pits or depressions larger than 150 nm in diameter. Counts of microvilli and especially pits were open to various interpretational errors. For this reason, counts were made in a blind fashion, random to experimental treatment. Pits were counted in a single session after all experiments were completed, since their counting criteria were found to evolve during the course of experimentation and in light of the transmission electron microscope findings.

These methods of quantification have some inherent limitations caused by factors such as inevitable cell junctions being included in the photographs, unusual convolutions of the cell surface, microvilli obscuring pits beneath them, clusters of interwoven microvilli, various qualities of image clarity, and varying degrees of tissue angle from the electron-collecting plate of the SEM.

RESULTS

The Normal Omental Surface

The omentum, a double sheet of mesentery bordered caudally by a fat strip, joins to the pancreas, spleen, and the stomach. Each sheet of the mesentery is composed of two layers of mesothelial cells which sandwich an irregular collagen meshwork. The sheets of mesentery are interrupted by fenestrations ranging in diameter from 5 to 50 μm (Fig. 1). Also present are foci of macrophages, lymphocytes, and mesothelial cells known as "milky spots." Mesothelial cells in and around these milky spots are morphologically distinct from those in the fenestrated regions. They display longer and more numerous microvilli in the normal condition, suggesting a different cellular microenvironment. In these experiments, only the cells of the fenestrated areas are considered.

The surface of the normal omentum, when viewed at low magnification with the SEM, appears smooth and velvety, and the borders of the mesothelial cells are clearly outlined by neat rows of microvilli that accumulate at the cell junctions (Fig. 2). On both sides of these junctions are broad zones, 3–4 μm wide, that are devoid of microvilli and serve to enhance the visibility of the cell borders. The rest of the cell is covered sparsely with microvilli. The microvilli are of typical diameter, 0.09 to 0.1 μm, and range in length from 0.2 to 1.0 μm. The number of microvilli on the surface of individual cells varies greatly, between 9 and 100/100 μm^2 with an average of 44/100 μm^2.

Interspersed among the microvilli, large surface

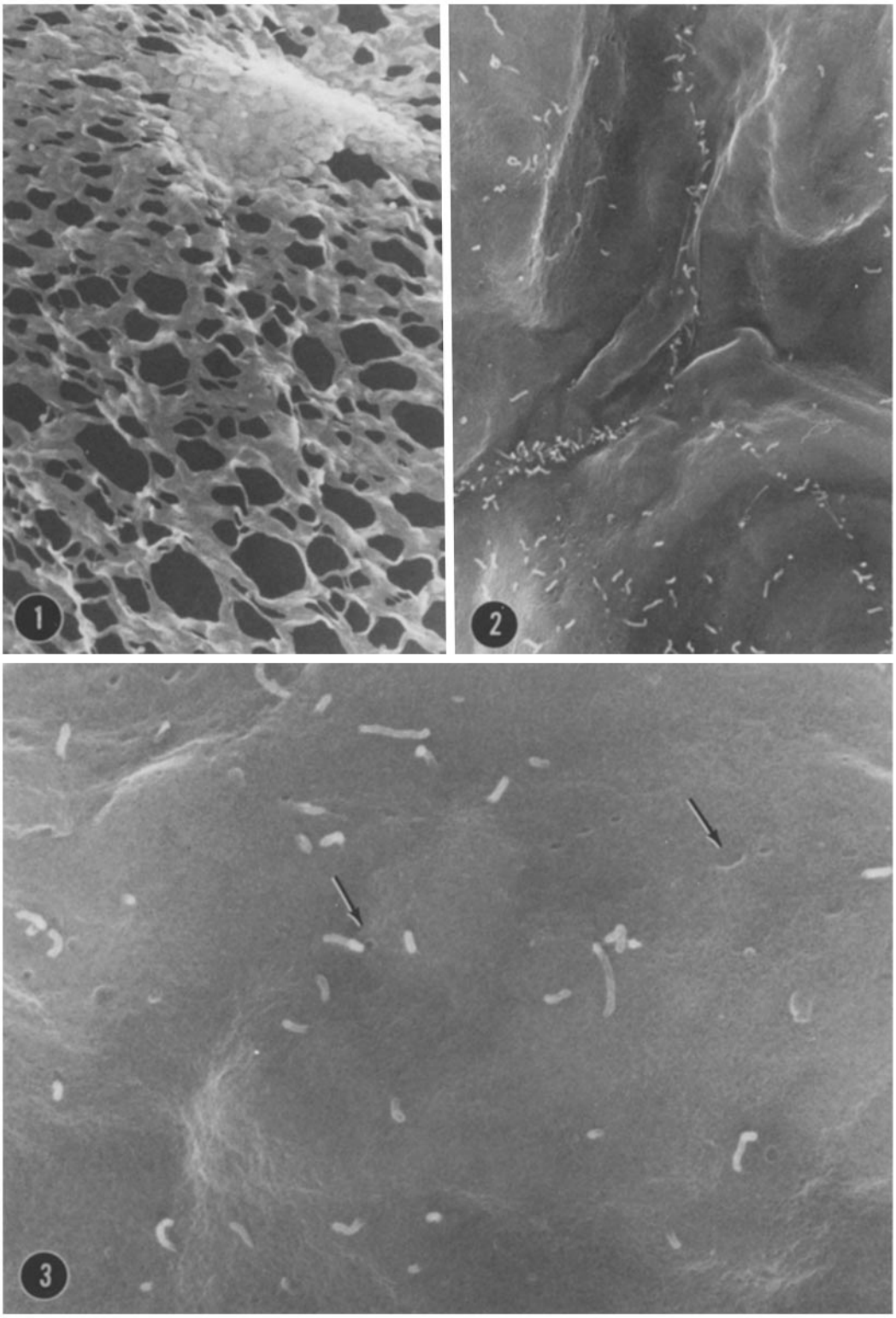
1
2
3

pits can be discerned (Figs. 3 and 8). The pits are seen by transmission electron microscopy to be composed of clusters of pinocytic vesicles whose openings empty into a common lumen or depression in the cell surface (Figs. 14, 15, 20, and 21). These structures, which will be shown to follow the same kinetics as microvilli, will be called "vesiculated pits." They have an average density on the cell surface of 30/100 μm^2 and range in size from 150 to 400 nm in diameter. In both normal and stimulated cells they are frequently in close association with the microvilli (Figs. 8, 12, 13, 16, 17, 20, and 21). Pits are restricted to areas of the cell surface containing microvilli; thus, in both normal and stimulated cells, areas of the surface that lack microvilli always lack pits. This is most evident in the clear zones at the cell junctions in normal cells (Fig. 2) and in cells where the distribution of microvilli is irregular (Fig. 13).

At high magnification, the cell surface appears to be composed of regular cobbles spaced ~30 nm, center-to-center (Figs. 10 and 17). An occasional, small, raised surface projection or nub is visible (Fig. 8). It is not clear at this time that the cobbles represent the true structure of the cell surface; they may result from fixation or other preparative procedures. The nubs, on the other hand, appear to represent authentic surface features since they increase in number after stimulation. Numerous depressed orifices in the cobbled surface mark the presence of pinocytic vesicles beneath (Figs. 8 and 10). The microvilli in favorable views display the same cobbled surface as the rest of the cell, and very rarely a larger nub protrudes from the lateral surface (Fig. 17). Visible at the bottom of the large vesiculated pits are regular openings of the same size and distribution as the openings of pinocytic vesicles (Fig. 15).

Changes in Omental Surface after Exposure to Serum

The surface of the mesothelial cell rapidly and dramatically alters when normal mouse serum is introduced into the peritoneal cavity (Fig. 4). The cell surface loses its smooth appearance and becomes rippled like the surface of a disturbed sea (compare Figs. 8 and 9). The regular cobbles are interspersed with many protruding nubbins ~40–70 nm in diameter, while the lateral edges of the microvilli display numerous and similar projecting nubs (Figs. 9, 11, and 20). The cell junctions, so clearly delineated in the normal condition, become almost completely obscured by the agitation of the surface and the numerous microvilli that now densely cover the cell.

The nature of surface features seen in scanning electron microscopy were clarified by transmission electron micrographs of thin sections of omentum. The close association of microvilli with pinocytic vesicles and large surface pits was confirmed (Figs. 16 and 20). It was clear that in many instances the membrane of the base of a microvillus also comprised a portion of the wall of an adjacent vesiculated pit or pinocytic vesicle (Figs. 16, 18, and 19). Also clarified was the nature of the large surface pits whose kinetics paralleled those of the microvilli. These vesiculated pits could be seen to open on both surfaces of the cell (Fig. 21), and some appeared to be entirely enclosed within it (Fig. 14).

Kinetics of Formation of Microvilli and Pits

When the morphologic nature of the reaction to serum was established, its quantitation was undertaken. It was found that the response to NMS on the one hand and to BSA or BGG on the other

FIGURE 1 The arrangement of mesothelial cells is shown in this overview of the dorsal sheet of the omentum. The larger areas between fenestrations were those selected for quantitative estimation of changes in microvilli and pits. A small milky spot, composed of mesothelial cells, macrophages, and lymphocytes is also shown. An occasional lone lymphocyte is seen attached to the fenestrated mesothelium. × 240.

FIGURE 2 The junction of three normal mesothelial cells is demarcated by accumulations of microvilli. There is typically a broad zone ~3–4 μm on both sides of the cell junction which lacks both microvilli and pits. Normal cells. × 4,000.

FIGURE 3 The normal omental mesothelial cell surface is sparsely covered with microvilli (average 44/100 μm^2) and with pits (average 30/100 μm^2). The surface is very smooth, and the openings of pinocytic vesicles can barely be discerned. The vesiculated pits (arrows) show a wide variation in size, suggesting various stages of formation. Normal cell. 0° tilt. × 12,000.

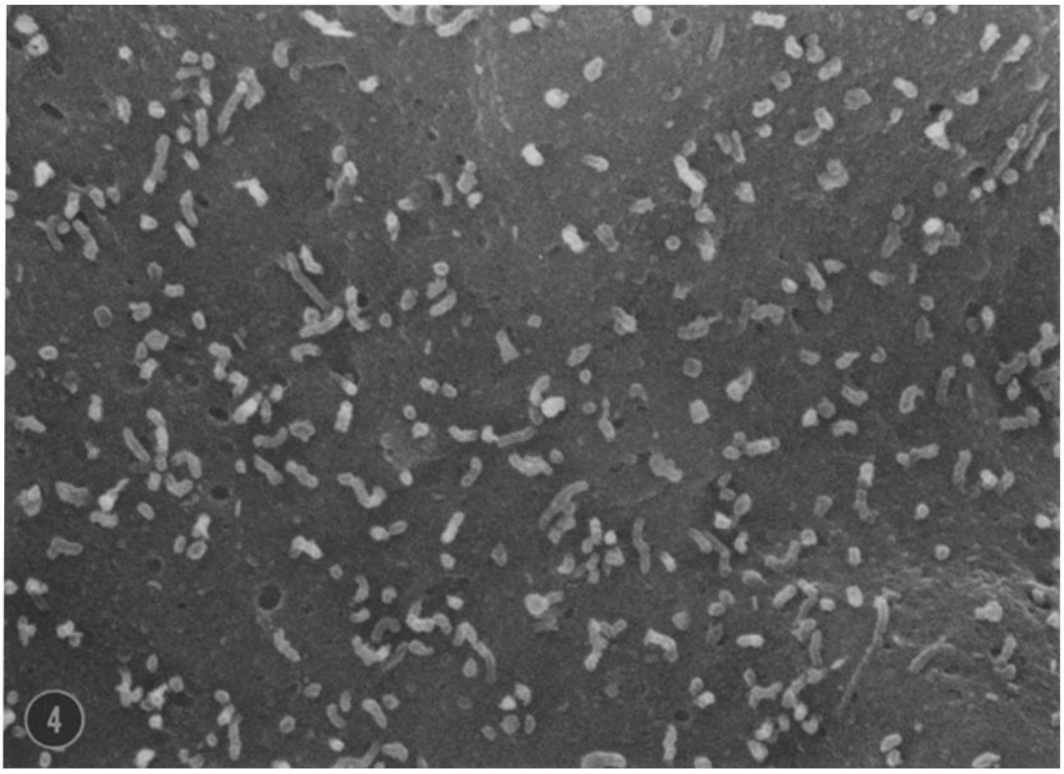

FIGURE 4 The NMS-treated mesothelial cell shows a dramatic increase in the density of microvilli and pits. An extensive stubble is also visible even at this moderate magnification. Cell treated for 30 min with NMS. 0° tilt. × 12,000.

produced quite different kinetics. Mouse serum, when introduced into the peritoneal cavity, produced a threefold increase in microvilli and pits as early as 2 min (Fig. 5 *A* and *B*). The increase was maximal at 30 min (sevenfold for microvilli and fourfold for pits), then declined, but even after 3 h the microvilli still averaged 175/100 μm^2 of surface. In contrast, BSA and BGG at protein concentrations equivalent to NMS (50 mg/ml) produced a different response; instead of increasing sharply, the number of microvilli and pits increased slowly to reach levels equivalent to NMS at 90 min (Fig. 5 *A* and *B*). The greatest contrast between the treatments was evident at 30 min when NMS caused maximal stimulation. While BGG appeared to be more effective than BSA in stimulating microvillus formation, the kinetics of the response to the two proteins were similar.

Heterologous serums were also tested for their capacity to stimulate the production of microvilli. Rat, rabbit, guinea pig, and fetal calf serum were somewhat less effective than isologous serum at 30 min (data not shown). Human serum (Fig. 22) also stimulated, but to a lesser degree.

The concentration of protein in the BSA solutions could be diluted 10-fold with no effect on the kinetics of the response (see Fig. 5 *A*) and diluted 50-fold with no effect on the 30-min response (see Fig. 22). On the other hand, when NMS was diluted 10-fold, the 30-min response was reduced by 50% to a level equivalent to that of BSA (Figs. 6 and 22). This suggested that whereas protein alone, as typified by BSA, could stimulate the appearance of microvilli, there might be single or multiple factors in serum which were much more effective. In exploration of what these supposed factors might be, two approaches were taken: first, mouse serum was fractionated on DEAE and CM cellulose and the various fractions were tested for activity and, second, in a series of experiments the effects of defined substances were examined.

Fractionation of Mouse Serum: Effect of Fractions

The decision made in fractionating the mouse serum was to determine whether there was a spe-

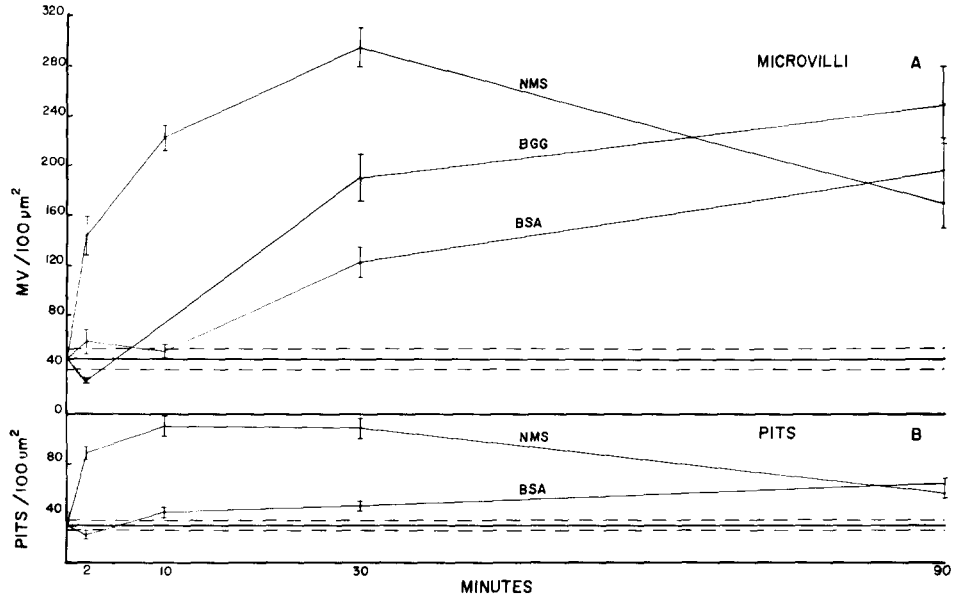

FIGURE 5 Graph showing numbers of microvilli (*A*) and vesiculated pits (*B*) per 100 μm^2 of mesothelial cell surface at various intervals after i.p. injection of NMS, BSA, or BGG. Each point for NMS and BSA represents the mean of counts from 15 photomicrographs, five from each of three omentums. Vertical lines indicate standard error of the mean. For BGG, each point represents 10 photomicrographs and two omentums. The mean and standard error of the mean of the normal cells are indicated by the horizontal line and dashed lines at the bottom of each graph. The protein concentration used was 50 mg/ml for NMS and BGG and 5 mg/ml for BSA. 50 mg/ml BSA produce 38, 108, and 170 microvilli/100 μm^2 at 2, 30, and 40 min. This represents identical kinetics. *MV*, microvilli.

cific protein involved in microvillus stimulation. Mouse serum was applied to a DEAE-cellulose column and processed as described in Materials and Methods. The pass-through and the eluate from the column were not concentrated but simply dialyzed against normal saline and filtered before testing in mice. Since the fractions represented a 33% dilution of whole serum, mice were also injected with 33% whole mouse serum to establish the level of stimulation at this concentration (22 mg protein/ml). Under these chromatographic conditions, all of the microvillus-stimulating activity applied to the column was recovered in the pass-through (Fig. 22). The proteins that were adsorbed and subsequently eluted from the column did not have activity (Fig. 22).

The DEAE pass-through was further fractionated on a CM-cellulose column. Before applying the pass-through to the column, the pH was lowered to 5.8 and the resulting precipitate was washed several times and stored at −20°C. The pass-through and eluate from the CM-cellulose column were dialyzed and filtered, and the precipitate was dissolved in normal saline and filtered.

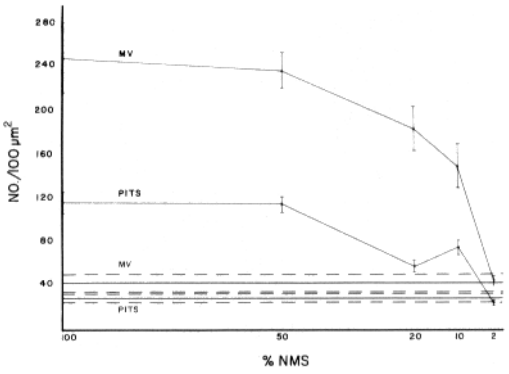

FIGURE 6 Effect of increasing dilution of NMS on the number of microvilli and vesiculated pits 30 min after injection. Each point and vertical bar represent the mean and standard error of the mean of 15 counts derived from two omentums. Normal values appear below as horizontal lines. Standard error of mean of normal values is within dashed lines.

These three fractions of the DEAE pass-through were then tested for microvillus-stimulating activity, and all had comparable activity at 30 min (Fig. 22).

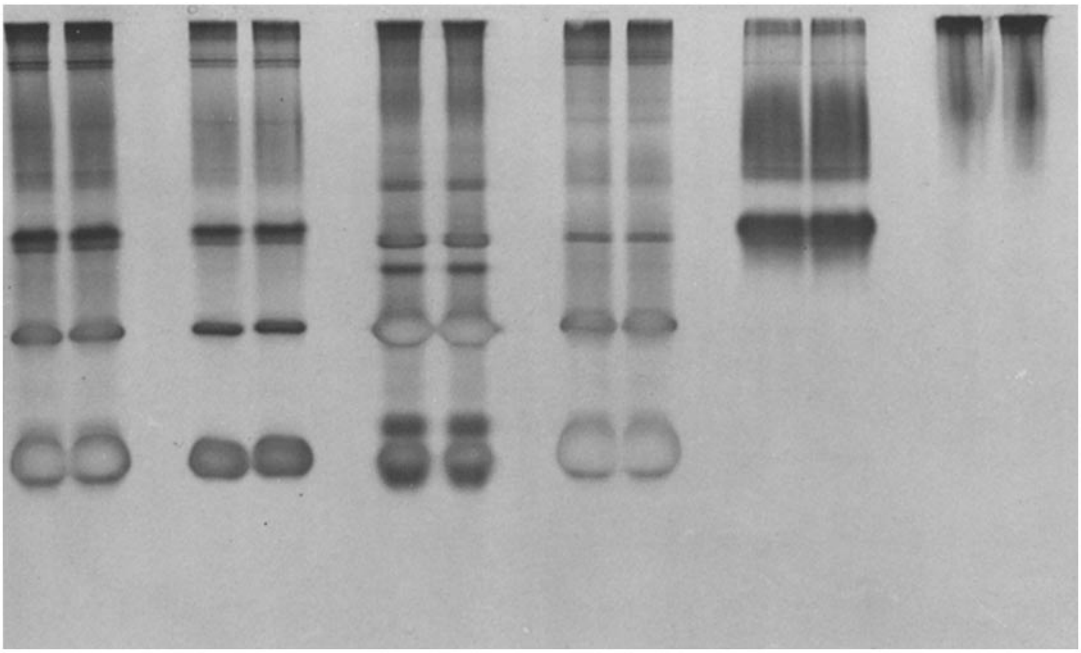

FIGURE 7 Electrophoresis of serum and chromatographic fractions on a 7.5% polyacrylamide slab gel. From left to right, the patterns represent, in terms of protein, 200 μg of NMS, 190 μg of DEAE-cellulose pass-through, 160 μg of DEAE-cellulose eluate, 170 μg of CM-cellulose pass-through, 165 μg of CM-cellulose eluate, and 190 μg of pH 5.9 precipitate. To permit visualization of minor proteins, the gel was overloaded with respect to some of the major proteins. The latter appear negatively stained on account of insufficient penetration of the dye through the concentrated protein bands.

Samples of the dialyzed fractions were applied to a polyacrylamide gel for examination of their protein components by electrophoresis (Fig. 7). The DEAE eluate, which represented 20% of the protein applied to the column, contained many protein species none of which stimulated microvillus formation. The removal of these inactive proteins from NMS resulted in an increase in microvillus-stimulating activity per milligram protein in the pass-through as compared to the activity

FIGURE 8 The normal cell surface, here rich in microvilli, shows the openings of pinocytic vesicles (arrow) that can be compared with the much larger openings of the vesiculated pits (asterisks). Microvilli partially obscure two of the pits, a common occurrence in both normal and treated cells. Note the smoothness of the cell surface, adorned by only occasional protruding surface nubs (arrowheads). Normal cell. × 36,000.

FIGURE 9 The cell treated with NMS is characterized by a roughened surface, by increased appearance of microvilli and pits, and greatly increased numbers of small nubs both on the surface of the cell and on the microvilli. Cell treated for 10 min with NMS. × 36,000.

FIGURE 10 At higher magnification, the surface of the normal cell is seen to be composed of homogeneous and even cobbles ~30 nm in diameter. Numerous pinocytic vesicle openings are visible as depressed orifices. The edges of the microvilli are slightly undulating but smooth. Normal cell. × 81,000.

FIGURE 11 The fine surface detail of the NMS-treated cell shows great alteration from the normal. There is a profusion of small nubs projecting from the surface, creating an agitated appearance. Many nubs decorate the lateral surface of the microvilli. Pinocytic vesicle openings are harder to see against the uneven background, but several are present (arrows). Cell treated for 10 min with NMS. × 81,000.

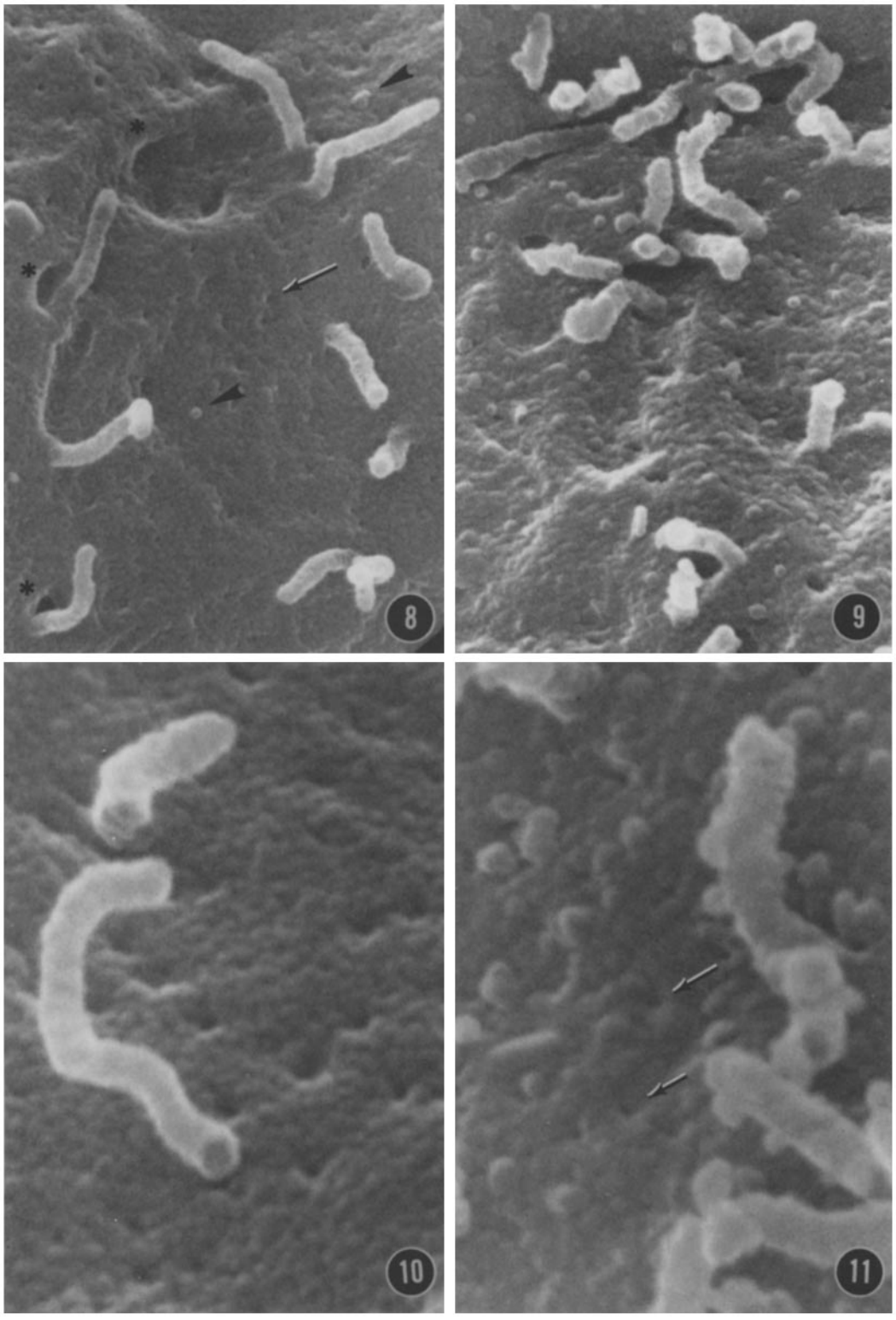
8
9
10
11

of the NMS applied to the column (Fig. 22: compare NMS 22 mg/ml to the DEAE pass-through, 19 mg/ml). Further, it was clear from the electrophoretic patterns (Fig. 7) and from a comparison of microvillus stimulation by the three fractions of the DEAE pass-through (*CM* in Fig. 22) that the stimulation was associated with more than one serum component.

Effect of Defined Substances on Microvillus Formation

Extensive dialysis of NMS did not reduce its efficacy in stimulating the appearance of microvilli. On the other hand, PBS reduced the number of microvilli on the cell surface, a phenomenon dubbed "saline wash-out." Glucose at concentrations ranging from 10 to 110 mM had no effect on microvillus density at 10 or 30 min. Human LDL (24), 0.2 mg/ml in 1 mg/ml BSA as carrier, did not increase microvillus density above that of the carrier at 30 min. In contrast, 5 μg/ml of insulin in 1 mg/ml BSA did increase the number of microvilli over that induced by the carrier. Purified human α_2-macroglobulin did not stimulate, but mouse myeloma proteins did. These pure immunoglobulin proteins, IgG (γlk), IgAk, and IgMk at 1 mg/ml, were appreciably more effective in stimulating microvillus formation than an equivalent amount of BSA (Fig. 22).

DISCUSSION

Although previous experiments have shown that microvillus density on the surface of cultured cells can be altered by a number of circumstances and treatments, the response has not been quantitated (2, 9, 10, 15, 16, 18, 22, 25, 26, 31, 33, 34). For the first time, quantitation of changes in the number of microvilli and pits on the surface of omental

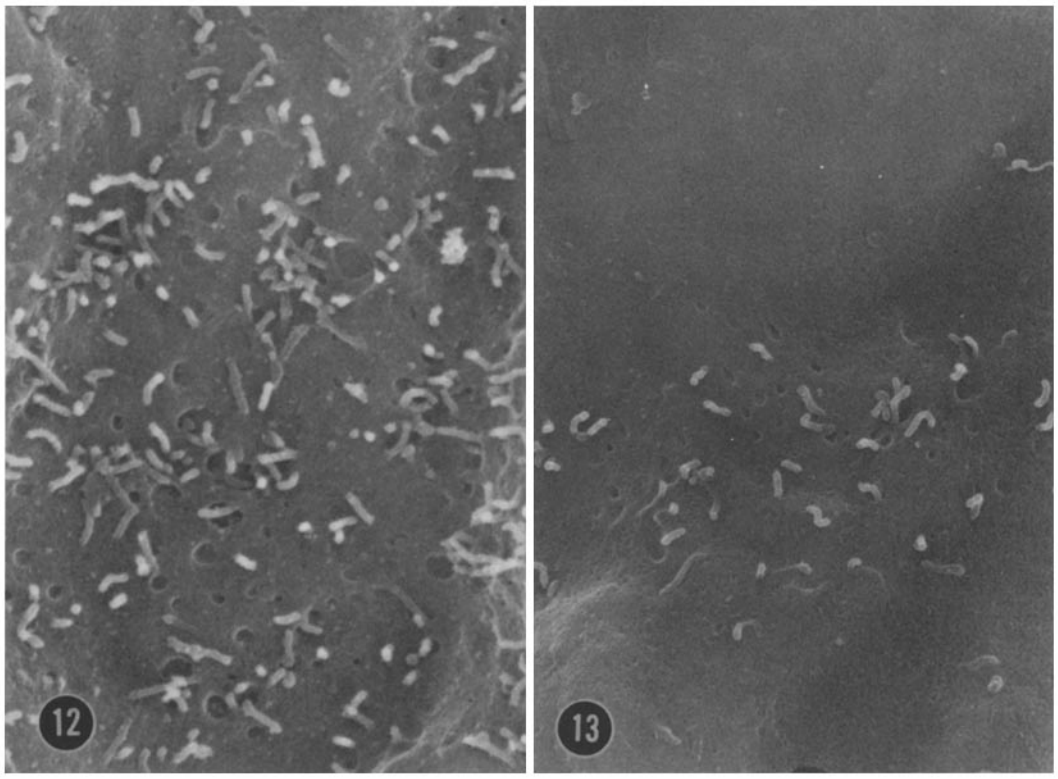

FIGURE 12 This cell shows an area of extensive pit formation and profuse accumulation of microvilli. The microvilli are in close association with the pits and sometimes even appear to emerge from them. Cell treated for 10 min with NMS. × 9,600.

FIGURE 13 The large surface pits are restricted to those areas of the cell having microvilli. No pits are present in areas bare of microvilli. Cell treated for 30 min with 10% NMS. × 9,360.

mesothelial cells provides for a description of their kinetics and a way of measuring the stimulatory effect of various substances. The response to isologous serum is immediate and it can be inferred from the kinetics data (Fig. 5 *A* and *B*) that microvilli and pits form in a matter of seconds after exposure to it. In contrast, the response to the purified proteins BSA and BGG is much slower. This difference in kinetics is unexplained, but several things suggest that it may be caused by an additive effect of several different components in serum. First, the stimulatory effect of serum is reduced by dilution, whereas that of BSA is not. Second, fractionation of serum shows the activity residing in the pass-through of the DEAE column to be distributed throughout the pass-through. Fi-

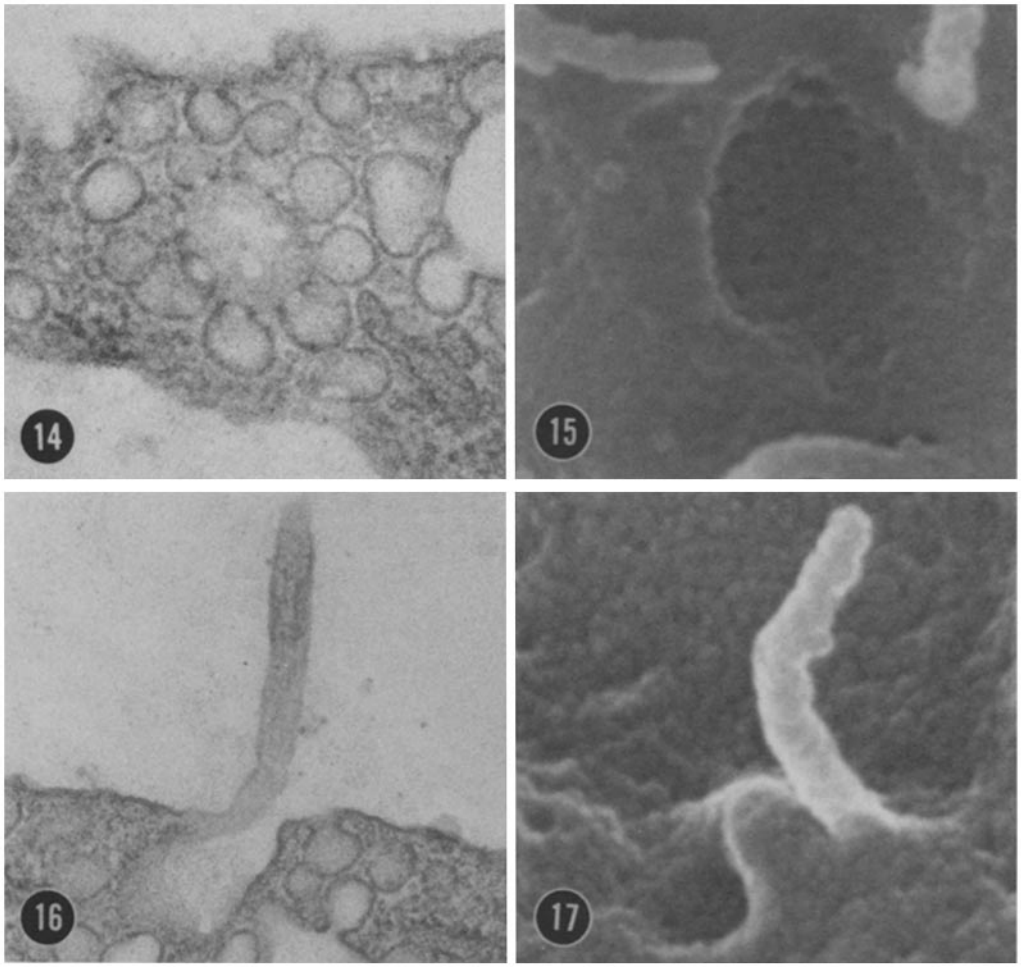

FIGURE 14 This thin section of a cell clarifies the nature of the large pit illustrated in Fig. 15. The relationship of the vesicles to the lumen of the vesiculated pit is clearly visible. The orifices of vesicles on the distal side of the pit and those surrounding the pit appear as pale circles against the wall of the pit itself. Cell treated for 30 min with NMS. × 64,000.

FIGURE 15 A high magnification view of the lower surface of a vesiculated pit reveals the presence of 20–30 pinocytic vesicle openings. Compare with Fig. 14. Cell treated for 10 min with NMS. × 64,000.

FIGURE 16 A cross-sectional view of the cell surface reveals the close proximity of a microvillus to the edge of a vesiculated pit. Normal cell. × 50,000.

FIGURE 17 This microvillus adjacent to a pit displays a lateral nub rarely seen on microvilli of normal cells. Normal cell. × 81,000.

nally, varieties of purified serum components were tested for their capacity to stimulate, and of these, insulin and the mouse myeloma proteins, IgG, IgA, and IgM gave significant stimulation. Glucose, LDL, and α_2-macroglobulin had no effect. The task of sorting out stimulatory factors is obviously complex and its execution could form the basis of a more extensive study.

Although the quantitative aspects of the increase in microvilli and vesiculated pits in response to serum stimulus and the variety of the components involved in stimulation are of interest, the cellular events themselves are of equal importance. The rapid and profound changes that occur in the mesothelial cell surface must reflect the function of the cytoskeleton of the cell, and it is to the cytoskeleton that future study of this phenomenon should also be directed. The combination of scanning and transmission electron microscopy has brought a new perspective to this cellular response. The vesiculated pits resemble structures previously illustrated in fat cells (32), vascular endothelium (32), smooth muscle cells (17), and noted in omental mesothelial cells (13). These pits, that were previously regarded as vacuoles or fused pinocytic vesicles, are now shown to be accumulations of vesicles opening into a common space that in turn has a single outlet to the cell surface. The structures are dynamic in that they wax and wane after stimulus with NMS and it is tempting to ascribe to them a role in transport of material across the cell since they can be seen to open on both sides of the cell. It is well known that materials injected into the peritoneal cavity are cleared very rapidly (6, 7) and that the omentum plays a part in this process (4, 5, 13, 30), but until the appropriate experiments are executed, the function of the vesiculated pits must remain unknown.

Among the functions ascribed to microvilli is that they serve as a site for membrane reserve (10, 15, 18). The results reported here appear directly to refute this hypothesis. After the stimulation of the cells with serum, there is an enormous increase in surface membrane as the result of vesiculated pit formation. At the time that this great demand is being made on the hypothetical membrane reserve of the cell, the microvilli do not decrease in number, but instead increase up to sevenfold. Thus, it appears that the membrane required for the formation of vesiculated pits does not occur at the expense of microvilli.

What, then, is the function of these labile microvilli? The restriction of microvilli and pits to certain regions of the cell, their physical association, and the similarity of their kinetics after stimulation indicate that there exists a correlation in their mobilization by the cell. This mobilization requires the rearrangement of substantial amounts

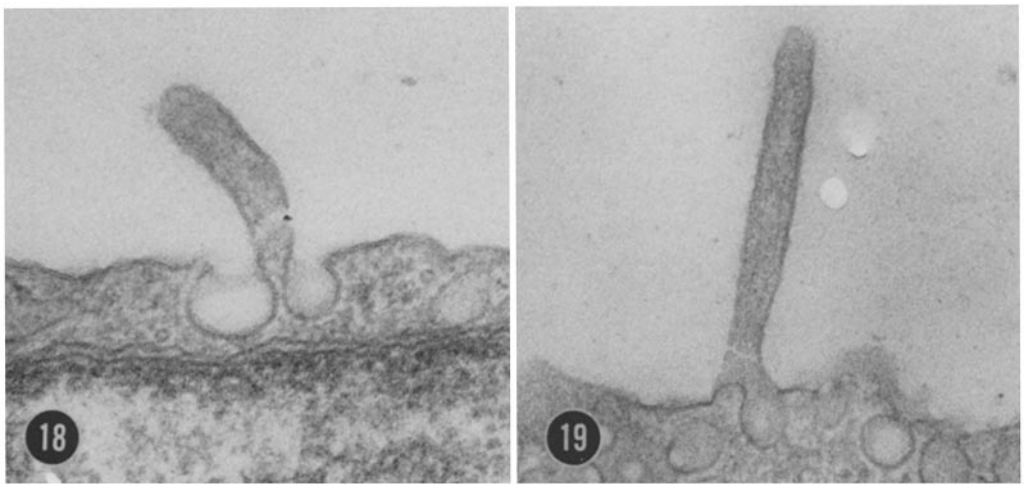

FIGURE 18 Microvilli can also assume a close physical association with the pinocytic vesicles themselves, as well as with the vesiculated pits. Here a microvillus is sandwiched between two pinocytic vesicles just above the nucleus of the mesothelial cell. Two microtubules cut in cross section are in the vicinity. Cell treated for 30 min with NMS. × 60,000.

FIGURE 19 An oblique section along a microvillus and an adjacent pinocytic vesicle illustrates the continuity of their surfaces. Cell treated for 30 min with NMS. × 54,000.

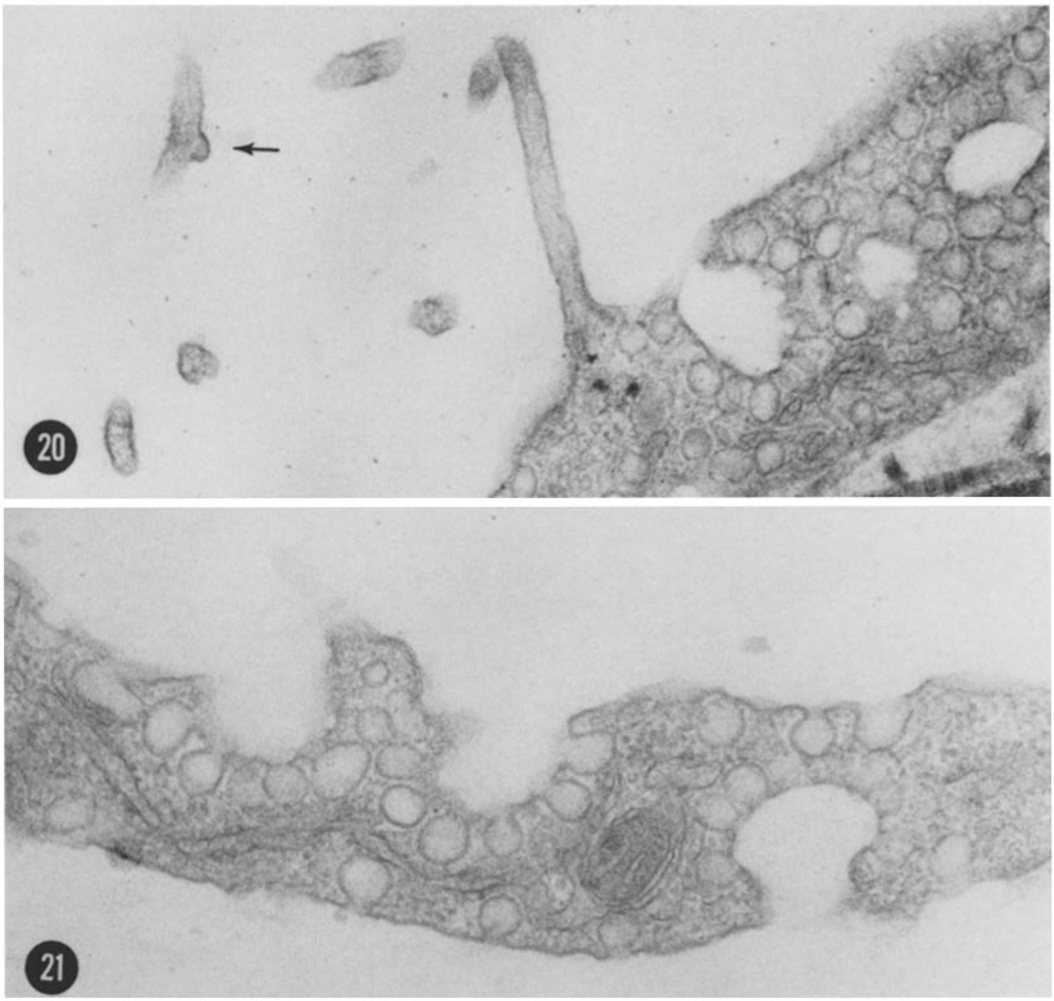

FIGURE 20 Many pits that open to the surface of the mesothelial cell are associated with microvilli. Others appear to be within the interior of the cell as illustrated by two of the three pits in this section. Collagen strands lie beneath the cell. Note also the presence of a nub, defined by unit membrane, on a glancing section of a microvillus (arrow). Such nubs are readily visible by SEM (compare with Fig. 11). Cell treated for 30 min with NMS. × 40,000.

FIGURE 21 Vesiculated pits are present on both sides of the mesothelial cell. The two pits at the left open on the peritoneal cavity. The pit at the right opens into the space between mesothelial cell layers. Cell treated for 30 min with NMS. × 45,000.

of membrane in a very short period of time. How does it occur? It can be hypothesized that labile microvilli function as the mechanism whereby the cell regulates the distribution of a subcortical layer of microfilaments which in turn may act to control movement of organelles to the cell surface. A close association between microvilli and the microfilaments of the contractile ring of dividing mouse embryo cells has already been described by Ducibella et al. (9). Microvilli disappear from the surface with the formation of the contractile ring and reappear when the subcortical band of filaments is dispersed. This relationship implied to Ducibella that there was some coordinated control over the surface topography and polymerization of cortical filaments. Microvilli of mesothelial cell are composed entirely of a more-or-less ordered meshwork of filaments; all other cell organelles

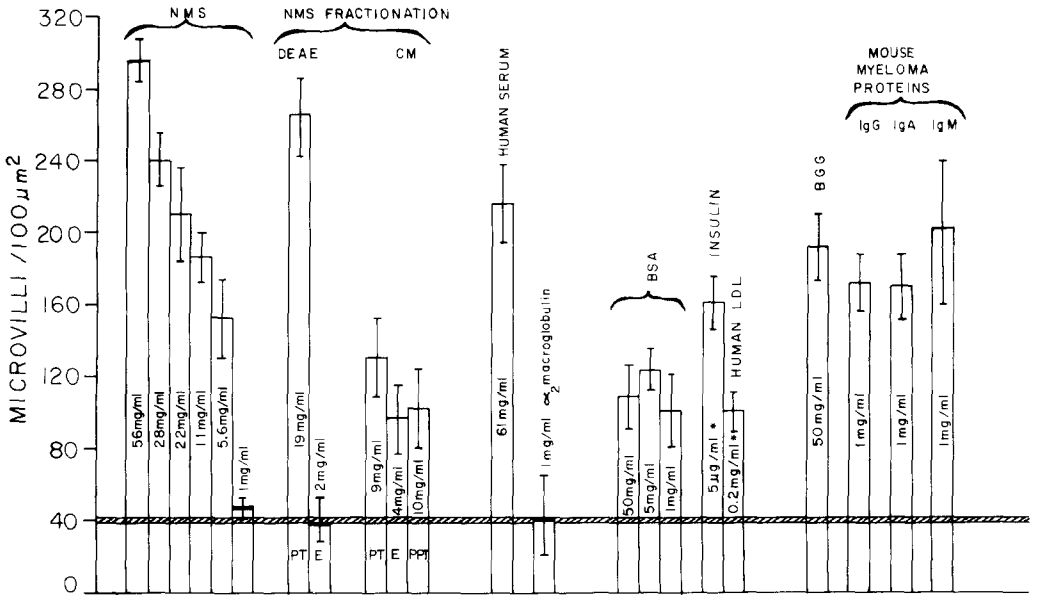

FIGURE 22 Microvillus density at 30 min after treatment. The bar graph shows the mean and standard error of counts from 10 photographs of one or two omentums for each treatment. The hatched line represents the average number of microvilli on unstimulated mesothelial cells. *PT, E,* and *PPT* refer to pass-through, eluate, and precipitate. Both insulin and LDL were injected with carrier protein and the level of stimulation should be compared with 1 mg/ml of BSA, the carrier protein.

are excluded (see Figs. 16–18). There is evidence (26, 27, 29) that filaments, presumably actin, form part of a cortical layer beneath the cell membrane and this layer, extending into microvilli, also excludes formed elements, e.g., mitochondria, ribosomes, and various vesicles, from the cell membrane. It has been proposed (1) that one of the functions of the subcortical microfilament network is to act as a "restraining cage" that prevents ready access of organelles to the cell membrane. The cell may regulate this restraining function by modulation of its microvilli. Thus, the sevenfold increase in microvilli that occurs 30 min after serum treatment could require movement of substantial amounts of filamentous material out of the cell cortex, thereby creating a local deficit in the subcortical "cage." Removal of this restraint by the formation of microvilli would not only facilitate the movement of membrane to the cell surface, presumably from the Golgi apparatus in the form of vesicles, but would also facilitate invagination of the vesiculated pits. It should be possible to test this hypothetical regulatory function of microvilli in other cell systems.

We are indebted to Dr. E. A. Peterson for his enthusiasm and for many helpful discussions. We also extend our thanks to Mr. Charles Mock for his assistance in performing the experiments and his skill in preparing the photographs and to Mrs. Anahid Ayrandjian for typing the manuscript.

Received for publication 28 August 1978, and in revised form 4 May 1979.

REFERENCES

1. ALLISON, A. C. 1973. The role of microfilaments and microtubules in cell movement endocytosis and exocytosis. *Ciba Found. Symp.* **14**:109–148.
2. AMOS, H., M. LEVENTHAL, L. CHU, and M. J. KARNOVSKY. 1976. Modifications of mammalian cell surfaces induced by sugars: scanning electron microscopy. *Cell.* **7**:97–103.
3. ANDREWS, P. M., and K. R. PORTER. 1973. The ultrastructural morphology and possible functional significance of mesothelial microvilli. *Anat. Rec.* **177**:409–426.
4. BUXTON, F., and J. C. TORREY. 1906. Adsorption from the peritoneal cavity. IV and V. The function of the omentum. *J. Med. Res.* **15**:55–87.
5. COTRAN, R. S., and M. J. KARNOVSKY. 1968. Ultrastructural studies on the permeability of mesothelium to horseradish peroxidase. *J. Cell Biol.* **37**:123–138.
6. COURTICE, F. C., and W. J. SIMMONDS. 1954. Physiological significance of lymph drainage of the serous cavities and lungs. *Physiol. Rev.* **34**: 419–448.
7. CUNNINGHAM, R. S. 1926. The physiology of the serous membranes. *Physiol. Rev.* **6**:242–277.
8. DAVIS, B. J. 1964. Disc electrophoresis. II. Method and application to human serum proteins. *Ann. N. Y. Acad. Sci.* **121**:404–427.
9. DUCIBELLA, T., T. UKENA, M. KARNOVSKY, and E. ANDERSON. 1977. Changes in cell surface and cortical cytoplasmic organization during early embryogenesis in the preimplantation mouse embryo. *J. Cell Biol.* **74**:153–167.
10. ERICKSON, C. A., and J. P. TRINKAUS. 1976. Microvilli and blebs as sources of reserve surface membrane during cell spreading. *Exp. Cell. Res.* **99**:375–384.

11. EVANS, R. B., V. MORHENN, A. L. JONES, and G. M. TOMKINS. 1974. Concomitant effects of insulin on surface membrane conformation and polysome profiles of serum-starved BALB/c 3T3 fibroblasts. *J. Cell Biol.* **61**:95–106.
12. FAWCETT, D. W. 1965. Surface specializations of absorbing cells. *J. Histochem. Cytochem.* **13**:75–91.
13. FEDORKO, M. E., and J. G. HIRSCH. 1971. Studies on transport of macromolecules and small particles across mesothelial cells of the mouse omentum. I. Morphologic aspects. *Exp. Cell Res.* **69**:113–127.
14. FELIX, M. D. 1961. Observations on the surface cells of the mouse omentum as studied with the phase-contrast and electron microscopes. *J. Natl. Cancer Inst.* **27**:713–745.
15. FOLLET, E. A. C., and R. D. GOLDMAN. 1970. The occurrence of microvilli during spreading and growth of BHK 21/C13 fibroblasts. *Exp. Cell Res.* **59**:124–136.
16. GEY, G. O. 1955. Some aspects of the constitution and behavior of normal and malignant cells maintained in continuous culture. *Harvey Lect. Ser. L.* 154.
17. HARMAN, J. W., M. T. O'HEGARTY, and C. K. BYRNES. 1962. The ultrastructure of human smooth muscle. I. Studies of cell surface and connections in normal and achalasia esophageal smooth muscle. *Exp. Mol. Pathol.* **1**:204–228.
18. KNUTTON, S., M. C. B. SUMNER, and C. A. PASTERNAK. 1975. The role of microvilli in surface changes of synchronized P8154 mastocytoma cells. *J. Cell Biol.* **66**:568–576.
19. LOWRY, O. H., N. J. ROSEBROUGH, A. L. FARR, and R. J. RANDALL. 1951. Protein measurement with the Folin phenol reagent. *J. Biol. Chem.* **193**:265–275.
20. MOOSEKER, M. S., and L. G. TILNEY. 1975. Organization of an actin filament-membrane complex. Filament polarity and membrane attachment in the microvilli of intestinal epithelial cells. *J. Cell Biol.* **67**:725–743.
21. ODER, D. L. 1954. Observations of the rat mesothelium with the electron and phase microscopes. *Am. J. Anat.* **95**:433–465.
22. O'NEILL, C. H., and E. A. C. FOLLET. 1970. An inverse relation between cell density and the number of microvilli in cultures of BHK 21 hamster fibroblasts. *J. Cell Sci.* **7**:695–709.
23. ORENSTEIN, J. M., and E. SHELTON. 1976. Surface topography of leukocytes *in situ*: cells of mouse peritoneal milky spots. *Exp. Mol. Pathol.* **24**:415–423.
24. ORCI, L., J.-L., CARPENTIER, A. PERRELET, R. G. W. ANDERSON, J. L. GOLDSTEIN, and M. S. BROWN. 1978. Occurrence of low density lipoprotein receptors within large pits on the surface of human fibroblasts, as demonstrated by freeze-etching. *Exp. Cell. Res.* **113**:1–13.
25. PORTER, K. R., D. PRESCOTT, and J. FRYE. 1973. Changes in surface morphology of Chinese hamster ovary cells during the cell cycle. *J. Cell Biol.* **57**:815–836.
26. PORTER, K. R., T. T. PUCK, A. W. HSIE, and D. KELLY. 1974. An electron microscope study of the effects of dibutyryl cyclic AMP on Chinese hamster ovary cells. *Cell.* **2**:145–162.
27. REAVEN, E. P., and S. G. AXLINE. 1973. Subplasmalemmal microtubules in resting and phagocytosing cultivated macrophages. *J. Cell Biol.* **59**: 12–27.
28. RESINER, A. H., P. NAMES, and C. BUCHOLTZ. 1975. The use of Coomassie Brilliant Blue G250 perchloric acid solution for staining in electrophoresis and isoelectric focusing on polyacrylamide gels. *Anal. Biochem.* **64**:509–516.
29. RUBIN, R. W., and L. P. EVERHART. 1973. The effect of cell-to-cell contact on the surface morphology of Chinese hamster ovary cells. *J. Cell Biol.* **57**:837–844.
30. SHIPLEY, P. G., and R. S. CUNNINGHAM. 1916. Studies on absorption from serous cavities. I. The omentum as a factor in absorption from the peritoneal cavity. *Am. J. Physiol.* **40**:75–81.
31. WESSELS, N. K., B. S. SPOONER, and M. A. LUDUENA. 1973. Surface movements, microfilaments and cell locomotion. *Ciba Found. Symp.* **14**:53–82.
32. WILLIAMSON, J. R. 1964. Adipose tissue, morphologic changes associated with lipid metabolism. *J. Cell Biol.* **20**:57–74.
33. WILLINGHAM, M. N., and I. PASTAN. Cyclic AMP modulates microvillus formation and agglutinability in transformed and normal mouse fibroblasts. *Proc. Natl. Acad. Sci.* **72**:1263–1267.
34. WILLOCH, M. 1967. Changes in HeLa cell ultrastructure under conditions of reduced glucose supply. *Acta Pathol. Microbiol. Scand.* **71**:35–45.